Gene mutation and biochemical characterization of recombinant mutant FtrB: A novel cupredoxin

Jessica Buchanan

Department of Chemistry, East Carolina University, Greenville, NC 27858, USA

12/07/2021

Abstract

Brucella is a Gram-negative zoonotic pathogen that is commonly passed from livestock to humans. The resulting condition, Brucellosis, is hard to diagnose, hard to treat, and chronic. *Brucella* is able to overcome the toxic environment of the host cell by utilizing various transport systems that steal essential nutrients, such as iron, from the host. The FtrABCD system of *Brucella* is an example of one of these transport systems involved in Fe^{2+} uptake and contributes to the high virulence of this bacteria. Periplasmic FtrB is hypothesized to be novel cupredoxin due to its common ancestry with known cupredoxins with a conserved Type-1 Cu binding site. However, FtrB does not conserve two His and a Cys Type-1 Cu coordinating residues seen in other cupredoxins. Previous homology modeling of wild-type *Brucella* FtrB shows Asp, Met, and His residues forming a putative Cu binding pocket. To test the proposed metal binding of these residues, single-site substitution mutants of FtrB (D55A, M81A, and H121A) were created. Isothermal Titration Calorimetry (ITC) results indicated greater binding affinity in the mutants than the wild-type protein. Circular Dichronic (CD) spectroscopy suggested significant structural differences for both mutants with H121A having more pronounced structural changes. The purpose of this study was to confirm the binding residues identified in the homology model bound Cu and mutations of these sites would eliminate Cu binding. Characterization assays performed on these mutants indicate structural and binding differences when compared to the wild-type.

Introduction

Brucella is a Gram-negative bacteria and is a known zoonotic pathogen (Pappas et al., 2005). The most common cause of human Brucellosis, the disease resulting from the infection of *Brucella*, is consuming unpasteurized dairy contaminated with the bacteria. However, some occupations that handle livestock can become infected through direct contact. In addition,

Brucellosis is one of the most common laboratory diseases due to its high virulence in its aerosolized form (Yagupksy & Baron, 2005). There is no defined set of symptoms associated with Brucellosis. In fact, most clinical symptoms have been linked to cases of Brucellosis. The most reported symptoms mimic those of the flu such as fever, fatigue, and myalgia (Solera et al., 1999). This disease is chronic and can undergo periods of relapse, even after treatment. Furthermore, Brucellosis is resistant to monotherapy treatments making it difficult to treat even when it is diagnosed. Some chronic cases have resulted in residual neurological syndromes after the body overcomes the infection (Murrell & Mathews, 1990).

According to a report by Gorvel and Moreno, once *Brucella* invades a host cell, it is engulfed by a macrophage, per the body's immune response. However, *Brucella* is able to overcome the toxic, acidic, environment within the macrophage by harboring inside a vacuole. In addition to creating a high acidity environment for the pathogen, the macrophage also attempts to starve the invader of essential nutrients (Gorvel & Moreno, 2002). One of these essential nutrients is iron. To overcome this hostile environment, *Brucella* has developed several different iron uptake systems that utilize various sources of iron from the host (Elhassanny et. al., 2013). In this acidic environment, most available iron is in its Fe^{2+} state. The first ferrous iron uptake system was the Feo system found in E. *coli*. This system has since been identified in *Bordetella*, another bacteria similar to *Brucella*. *Bordetella* also has a novel ferrous iron transport system of its own named the FtrABCD system after the four components it's comprised of. It is the only known ferrous iron transport system that is proposed to utilize a four component Cu-dependent redox mediated iron uptake mechanism. Preliminary studies performed by Armstrong and colleagues on *Bordatella* suggest all four gene are involved in FtrABCD's function and that the system functions to uptake ferrous iron. In *Bordetella,* FtrA is hypothesized to be a P19-type protein, FtrB is a proposed novel

cupredoxin, FtrC is predicted to be a iron permease homologue, and FtrD is thought to oxidize FtrB's bound copper to reset the mechanism (Armstrong & Brickman, 2012). The proposed structure of the FtrABCD system and proposed function of each component is shown in Figure 1.

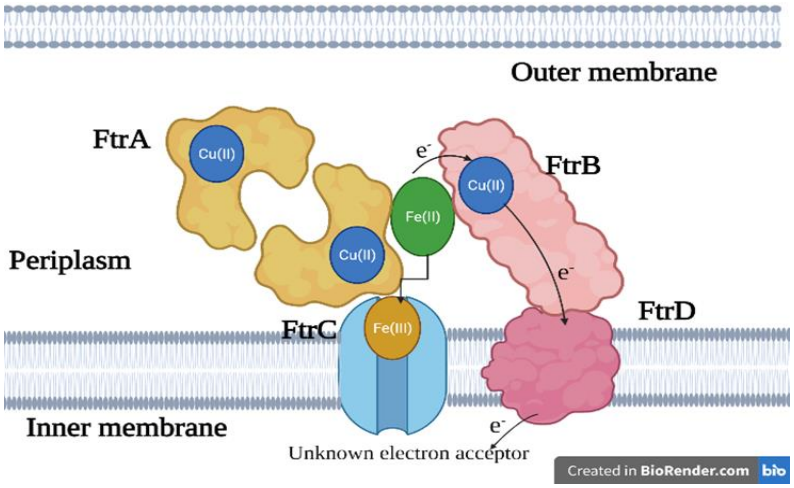

Figure 1: Proposed location of each FtrABCD component. The transport mechanism of the Fe^{2+} ion is shown as well as the electron exchange of the redox mediation.

According to Elhassanny and colleagues, iron uptake has also been experimentally shown to affect virulence in *Brucella*. In this study, the group characterized FtrA in B. *abortus*. The results support their hypothesis that FtrA is a P19-type protein. In medium with low iron ability, FtrA mutants only utilized haem as a source of iron. This was more pronounced with a pH 6.0. In a mouse model, mutants showed decreased function compared to the parent strain suggesting the pathogen needs ferrous iron in a mammalian host. In addition, results of these studies concluded FtrA has metal binding domains predicted to contribute to iron binding. The authors of this study analyzed the amino acid sequence of FtrABCD and predicted FtrA to be sent to the periplasm, FtrB to the periplasm surface of the inner membrane, and FtrC & D are incorporated into the inner membrane. These proposed locations support the proposed function of each component (Elhassanny et. al., 2013).

FtrB is the next component needing to be characterized in the system. FtrB is hypothesized to be a novel cupredoxin with unique Type-1 Cu^{2+} binding site with unidentified residues. In the proposed mechanism, FtrB oxidizes Fe^{2+} as it transports it through FtrC. Preliminary studies on wild-type FtrB indicate a β-sheet folding characteristic of known cupredoxins (unpublished data, Kerkan *et al)*. ITC analysis of apo wild-type FtrB indicate 1:1 (protein:Cu^{2+}) binding with low μM affinity (unpublished data, Kerkan *et al*). Furthermore, ITC studies on Cu^{2+}-saturated wild-type FtrB show 1:2 (protein:metal) Mn^{2+} (a mimic of Fe^{2+}) affinity. Ferrozene assays performed on wild-type FtrB showed the protein displays ferrous oxidase properties (unpublished data, Kerkan *et al*). The results of these studies support the hypothesis that wild-type FtrB is a novel cupredoxin.

Homology models of wild-type FtrB show His121, Met81, and Asp55 forming a proposed Cu^{2+} binding pocket, as seen in Figure 2 (unpublished data, Kerkan *et al*). In this study, H121A, M81A, and D55A mutants were constructed through site directed substitution mutagenesis on pET28(a)-TEV containing FtrB and were expressed through E. *coli* BL21 cells. CD and ITC studies were performed on H121A and D55A to determine secondary structure and metal binding affinity, respectively. Both mutants showed a change in secondary structure higher Cu^{2+}affinity compared to wild-type FtrB. Although these mutations did not limit Cu^{2+} binding as hypothesized, Mn^{2+} affinity and the ability of the mutants to oxidize Fe^{2+} needs to be confirmed in future studies.

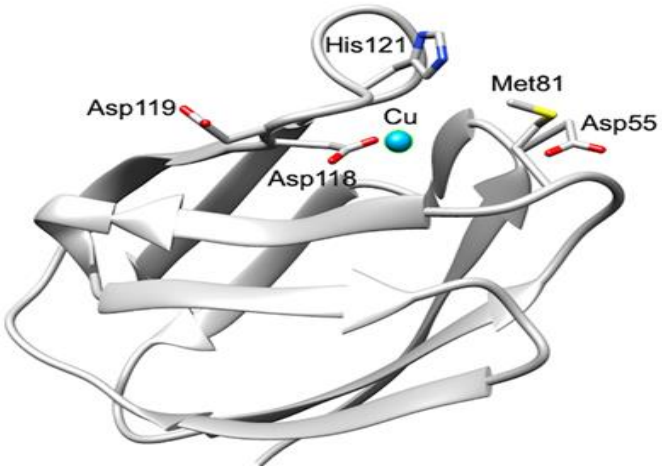

Figure 2: Homology model of wild-type FtrB showing proposed Cu^{2+} binding sites His 121, Met81, and Asp55.

Experimental

FtrB Mutagenesis

The amino acids predicted to influence Cu^{2+} binding were sequenced and mutation sites identified to change them to an alanine. NEBaseChanger software was used to design mutagenic oligonucleotide primers, Figure 3, that changed the codons for D55A, M81A, and H121A. The pET28(A)+TEVftrB vector, Figure 4, used in prior FtrB studies (unpublished data, Kerkan *et al*) was used as the starting material for mutagenesis. The Q5 Mutagenesis Kit from New England Biolabs was used to perform site directed mutagenesis according to the kit's protocol. The primers, template plasmid, and Q5 Hot Start High-Fidelity 2X Master Mix were combined in polymerase chain reaction (PCR) tubes. The reaction mixtures were placed in a thermocycler to undergo PCR amplification and obtain linearized DNA fragments containing the target mutations. The PCR product was then circularized using the Q5 KLD Enzyme Mix and incubating the reaction for five minutes at room temperature. The circularized product was then transformed into E. *coli* DH5α. These cells were plated onto Luria Broth (LB)-agar plates containing 45μg/mL kanamycin (kan).

Kanamycin was chosen because the vector used for cloning has a natural resistance, making it ideal for targeting unwanted bacteria. Samples of the transformants were sequenced to confirm successful mutations. Plasmid DNA from the confirmed mutants was transformed into E. *coli* BL21DE3 for protein expression.

Mutant	**Forward Primer Sequence**	**Reverse Primer Sequence**
D55A	GAGTTCAAGGcCGGGGTTATCAC	AAGGCGAAACGTTGGCTC
M81A	TACGGGCTCAgcGCCAGCGGAG	TTAACCAGCTCGATGCGG
H121A	CGATGATTTTgcTCCCGGTGGTAC	AAGAACGGATATTCGCCC

Figure 3: Table containing the oligos designed for substitution mutation. The upper-case indicates target-specific primers. The point of mutation is highlighted.

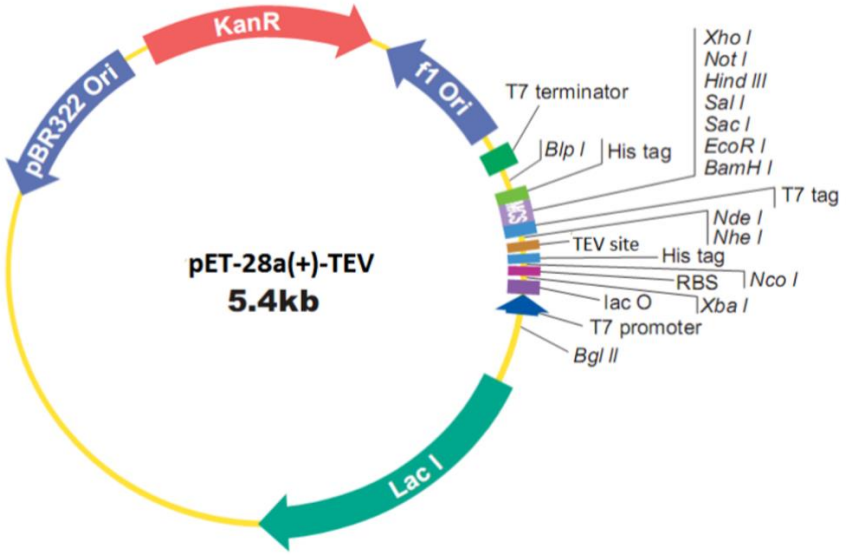

Figure 4: pET-28(a)-TEV vector containing ftrB. Vector shows Kanamycin resistance and a Lac operon.

FtrB mutant protein expression and purification

E. *coli* BL21DE3 cells containing the pET28(a)+TEV vector carrying the *ftrB* mutants encoding H121A, D55A, and M81A amino acid changes were streaked on to LB-agar plates with kan (45μg/mL) added and incubated over night at 37ºC. An individual colony was used to inoculate LB supplemented with kan and incubated overnight with shaking. This culture was used to inoculate one liter of Terrific Broth with kan (45μg/mL). The culture was left to grow for approximately four hours at 37ºC or until the optical density at 600nm reached 0.8. IPTG (2mM final concentration) was then added to the culture in order to induce protein expression and the culture allowed to incubate for another four hours at 37ºC. The cells harvested by centrifugation at 6,000xG at 4ºC for thirty minutes. The resulting pellets were stored at -80ºC until the protein could be purified.

The frozen pellet was resuspended in approximately 40mL His-wash buffer (50mM sodium phosphate, 300mM sodium chloride, 10mM imidazole; pH 7.4). The cells were put through a French press in order to lyse them. Cells were passed through an ice-cold French Pressure Cell at 5,000psi three times. The resulting lysate was centrifuged at 17,000xG at 4ºC for 20 minutes. Samples of the cleared lysate and insoluble pellet were taken for SDS-PAGE gel electrophoresis (SDS). The cleared lysate was added to a HisPur^{TM} Cobalt Resin Column from ThermoFisher according to manufacturer's instructions. The lysate was allowed to flow through the cobalt column at a rate of about 0.5mL/minute, and a sample of the flow through was taken for SDS. His-wash buffer (two bed volumes) was used to rinse the column and a sample taken for SDS. The protein containing a His-tag was eluted using three bed volumes of His-elution buffer (50mM sodium phosphate, 300mM sodium chloride, 150mM imidazole; pH 7.4) and a sample taken for SDS. The eluted protein was dialyzed twice for two hours and then over night with His-wash buffer

to remove remaining imidazole. The protein was then digested at room temperature over night with TEV and β-marcaptoethanol to remove the His-tag. The isolated protein was then ran over the Co-column again to remove the tag. A sample of isolated protein was saved for SDS, and the rest was dialyzed in 10mM Aces Buffer at pH6.4 to be stored until characterization could be performed.

Biochemical characterization of D55A and H121A

Isothermal Titration Calorimetry (ITC) and Circular Dichroism (CD) analysis was performed on H121A and D55A mutants. For ITC analysis, the proteins as isolated were prepared at a concentration of 55μM in 100mM HEPES buffer and 100mM NaCl, pH 7.3. Each sample was titrated with 0.5mM Cu^{2+}. Injections were 200s apart with a stirring speed of 400rpm and temperature of 25ºC. For CD analysis, the proteins were buffer exchanged with PBS pH 7.3 to a 50mM concentration of protein. A 300μL sample was used for analysis in a 1.0mm cuvette.

Results

Mutagenesis and purification of D55A, M81A, and H121A

All protein mutagenesis was successful in producing viable mutations to analyze. Duplicates of each mutation were made to help ensure at least one positive mutation. Sequencing performed on the mutants confirmed this, as seen in Figure 5 with the mutation sites highlighted. Only one of the M81A mutations did not yield a positive clone. However, the other sample sent for sequencing was a positive clone and was therefore viable for use in the study.

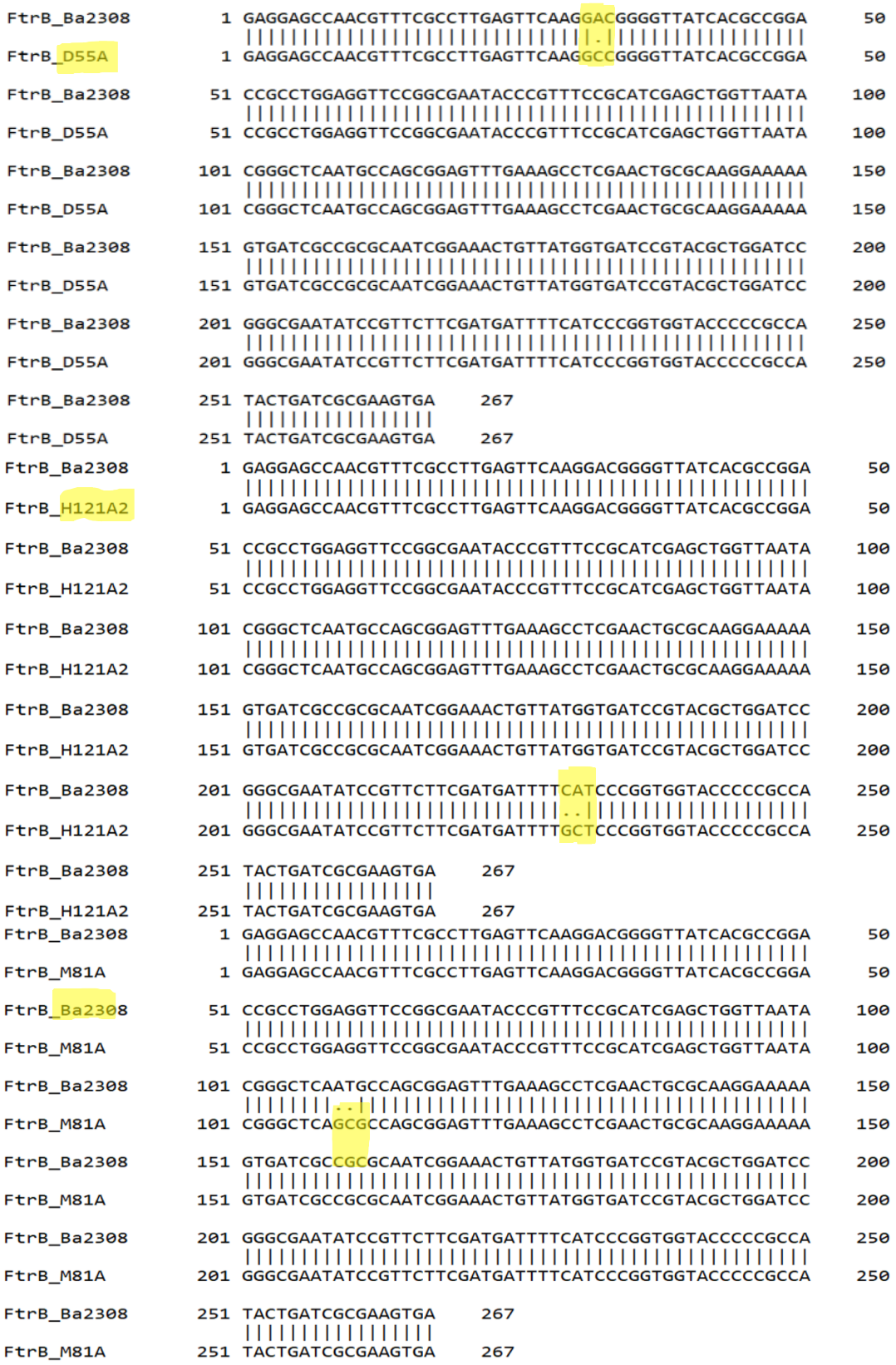

Figure 5: DNA sequencing of D55A, H121A, and M81A mutants indicating positive mutation. The site of mutation is highlighted.

During the purification of the proteins, M81A was the only mutation to not be successfully recovered. SDS was performed using the samples taken from each step of the purification process to gain insight into where the protein was lost. These results, Figure 6, show that the protein was not extracted from the pellet during the French pressing of the cells. The other two proteins were successfully purified and stored to be used in the characterization assays.

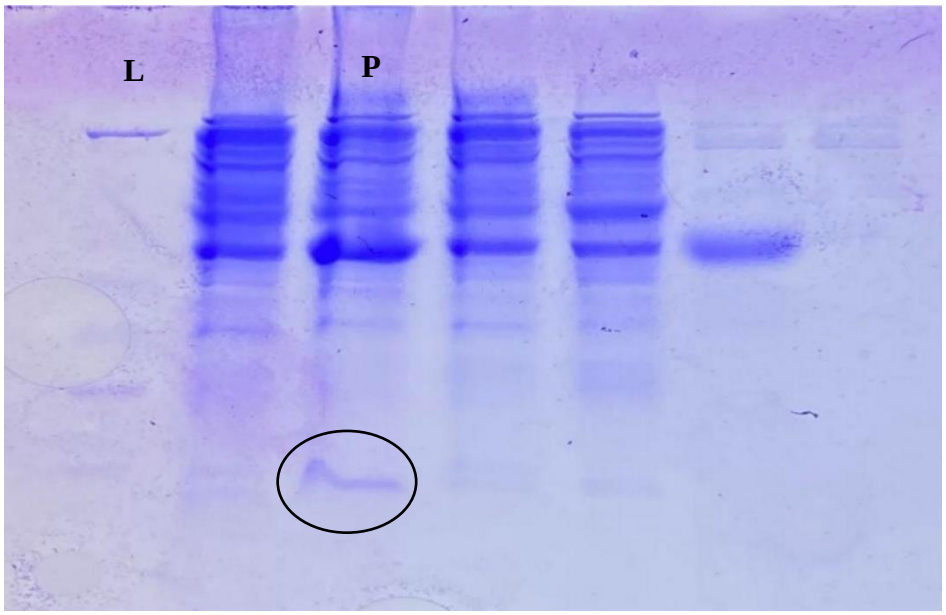

Figure 6: SDS-PAGE gel electrophoresis of M81A samples taken throughout the purification process in the order previously listed. The first lane is a 1K $^{+}$ladder (L), and the third lane is the sample collected from the pellet (P) formed from centrifuging the French pressed product. The protein trapped in the pellet is circled.

Cu^{2+} binding affinity and secondary structure of D55A and H121A

CD analysis of the H121A mutant, Figure 7, resulted in inconclusive evidence of the secondary structure. The shape of the spectrum suggests α-helix folding, however the intensities of the peaks are positive whereas α-helices are known to have negative intensities. Therefore, the secondary structure of the mutant cannot be determined, merely that it is significantly different from the definite β-sheet structure of wild-type FtrB seen in earlier studies performed by Kerkan

and colleagues. ITC data from the H121A mutant, Figure 9, supports this. The Cu^{2+} affinity of both mutants was found to be 1:1.5 (protein:metal) compared to wild-type FtrB that was reported as having 1:1 (protein:metal) binding (unpublished data, Kerkan *et al*).

Though CD analysis of the D55A mutant, Figure 8, confirmed β-sheet folding, the spectrum of the mutant had a much broader band than wild-type FtrB spectrum generated by Kerkan and colleagues. The average structure of these two spectra was similar with the only significant difference being the sharpness of the band. ITC results for D55A, Figure 10, corresponds with this data. The Cu^{2+} affinity of the mutant being higher than the wild-type could indicate structural change.

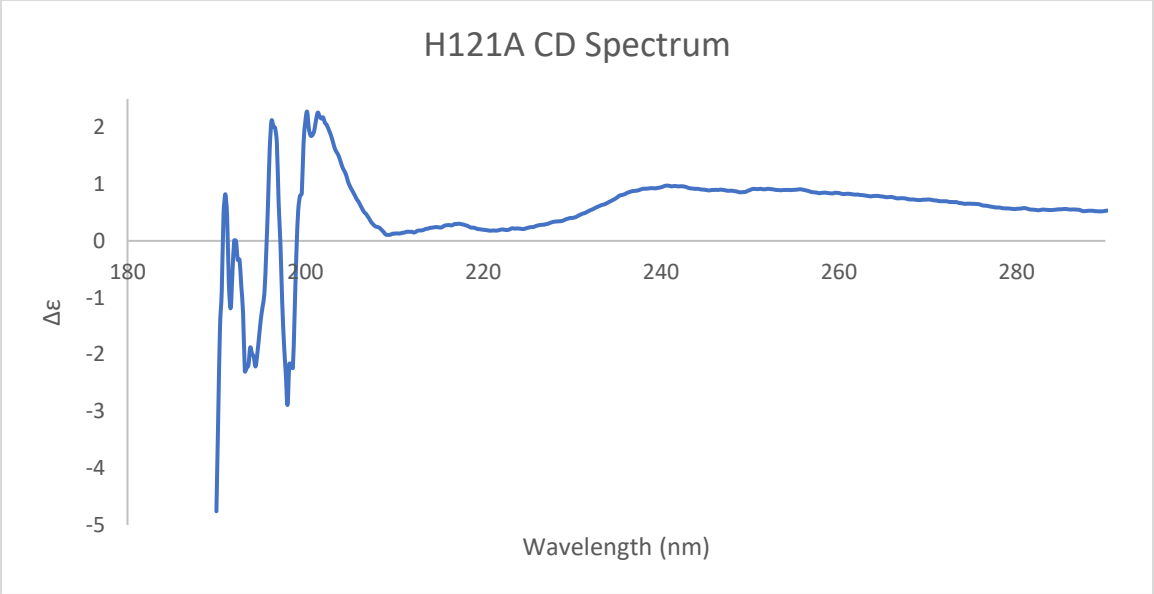

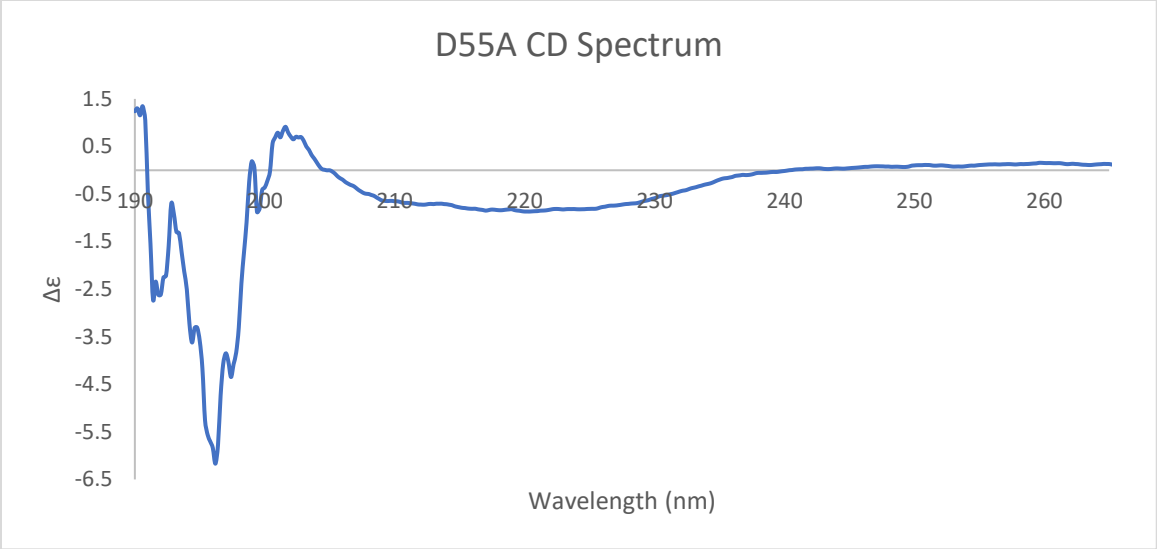

Figures 7 & 8: CD spectra of H121 and D55 mutants. The proteins were buffer exchanged with PBS pH 7.3 to be analyzed. 300μL of sample was used in a 1.0mm cuvette.

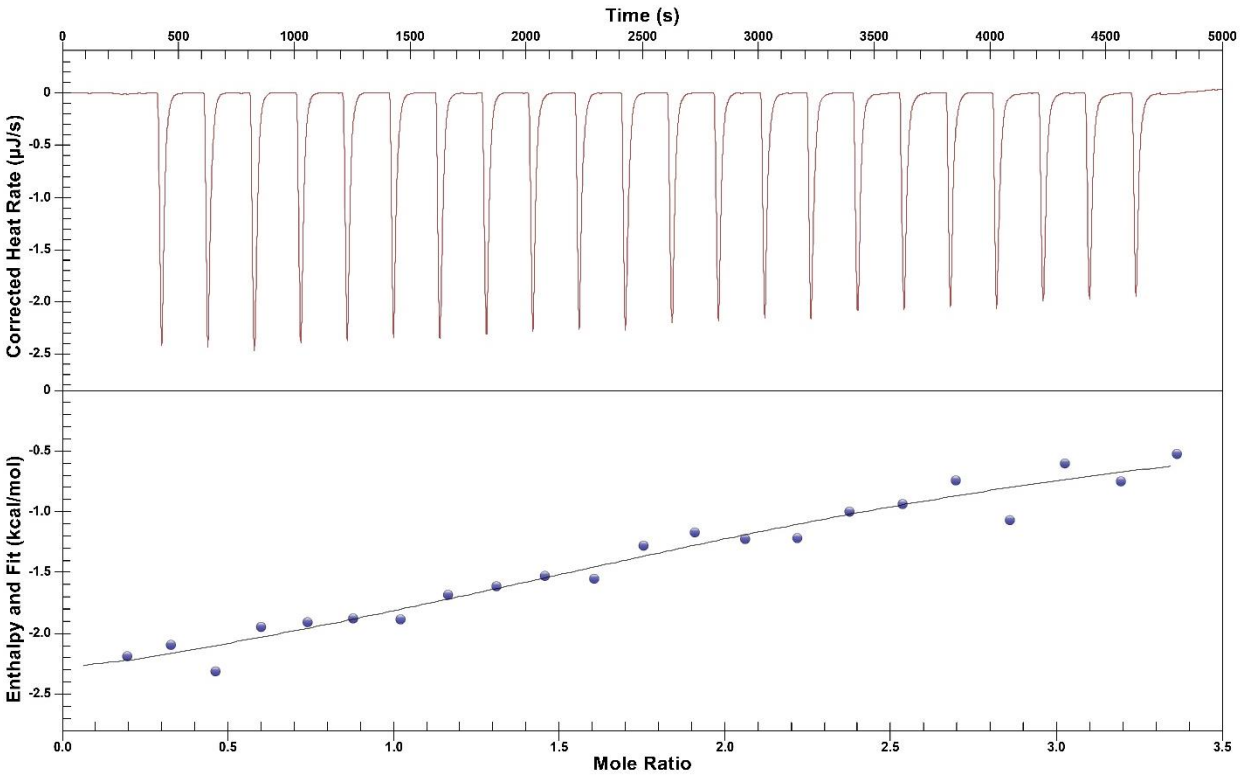

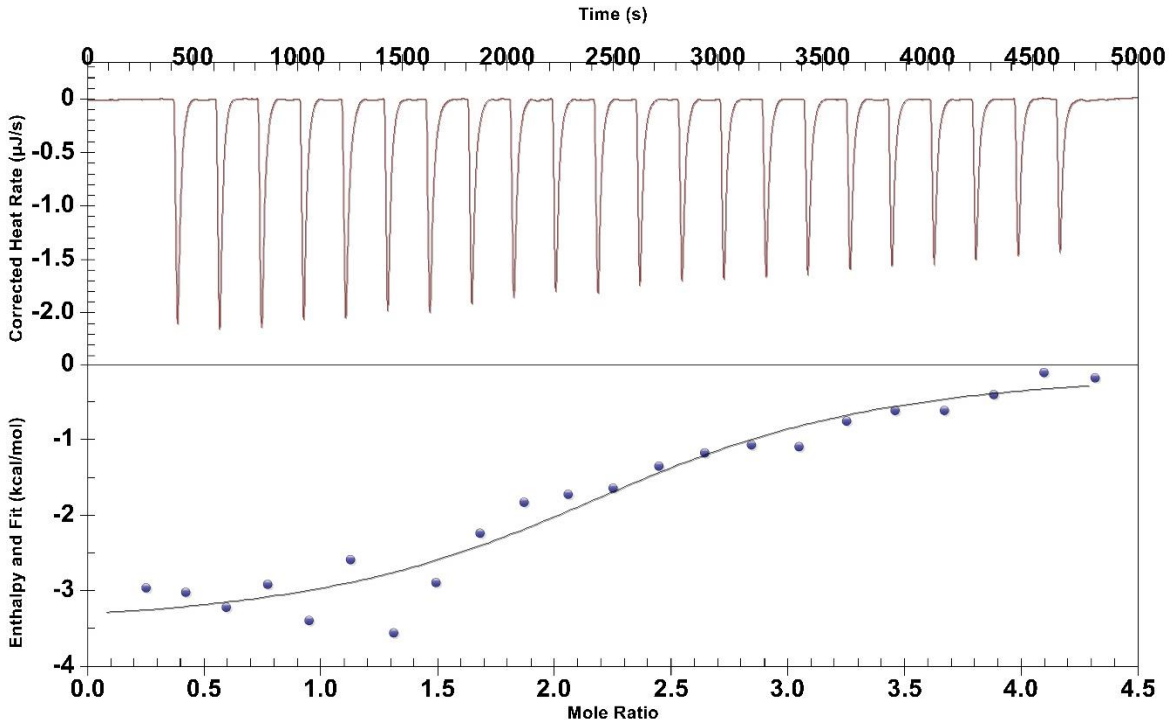

Figures 9 & 10: ITC nanograms of H121A and D55A, respectively. The proteins were prepared at a concentration of 55µM in 100mM HEPES buffer and 100mM NaCl, pH 7.3. Each sample was titrated with 0.5mM Cu^{2+}. Injections were 200s apart with a stirring speed of 400rpm and temperature of 25°C.

Discussion

It is hypothesized that the reason the M81A protein was not able to be purified is because the mutation caused significant misfolding and was no longer soluble. The SDS results of M81A support this by identifying the protein in the insoluble pellet sample rather than the cleared lysate sample. This may indicate that the M81 residue is critical for proper folding of the protein. Further research is needed to validate this hypothesis and determine if these genes play a role in Fe^{2+} uptake.

The ITC results indicate that the mutations were still able to bind Cu^{2+} and at a higher rate than the wild-type. For H121A, this could mean that the structural difference of the mutant caused

other metal binding sites to be exposed, increasing affinity. However, future studies need to be performed to confirm this hypothesis. For D55A, these results suggest that this site is not the most important Cu^{2+} binding site in the protein. Further ITC studies need to be performed to provide clarification on the binding properties of the mutants by comparing these as-isolated results with results from apo-mutant trials.

CD results for H121A did not offer conclusive evidence to determine secondary structure. Literature research on α-helix presentation in CD spectra could provide insight into why the suspected α-helix shape of the mutant spectrum had a positive intensity. The definite folding disparities between the H121A mutant and wild-type FtrB could relate to H121 being the only proposed binding residue that is conserved in all known cupredoxins. If FtrB is a cupredoxin as proposed, it is reasonable that mutating a site conserved in all cupredoxins would significantly alter the protein's structure. Though the D55A mutant displayed β-sheet folding like wild-type FtrB, the significant difference in band width could indicate some level of structural change. However, further studies are needed to determine the location of these structural differences.

The purpose of this study was to determine if mutants of proposed Cu^{2+} binding residues would still be able to bind Cu^{2+} and if these mutations caused changes in the protein's secondary structure. Results of this study indicate that the mutations of these binding residues affected Cu^{2+} binding but did not limit it as expected. The secondary structure of the mutants were also significantly different from wild-type FtrB, but the exact structural differences could not be determined. Future studies can use these results as a starting point for further work on characterizing FtrB. These studies could include testing the Mn^{2+} (Fe^{2+} mimic) affinity as well as the ferrous oxidizing properties of these mutants.

References

Armstrong, S. K., Brickman, T. J., & Suhadolc, R. J. (2012). Involvement of multiple distinct Bordetella receptor proteins in the utilization of iron liberated from transferrin by host catecholamine stress hormones. *Molecular microbiology*, *84*(3), 446-462.

Banerjee, S., Garrigues, R. J., Chanakira, M. N., Negron-Olivo, J. J., Odeh, Y. H., Spuches, A. M., ... & Dasgupta, S. (2020). Investigating the roles of the conserved Cu2+-binding residues on Brucella FtrA in producing conformational stability and functionality. *Journal of Inorganic Biochemistry*, *210*, 111162.

Chan, A.C.K., Doukov, T.I., Scofield, M., Tom-Yew, S.A.L.,Ramin, A.B., Mackichan, J.K.,et al. (2010) Structure andfunction of P19, a high-affinity iron transporter of the human pathogen Campylobacter jejuni.J Mol Biol401:590–604.

Elhassanny, A. E., Anderson, E. S., Menscher, E. A., & Roop, R. M. (2013). The ferrous iron transporter FtrABCD is required for the virulence of B rucella abortus 2308 in mice. *Molecular microbiology*, *88*(6), 1070-1082.

Gorvel, J. P., & Moreno, E. (2002). Brucella intracellular life: from invasion to intracellular replication. *Veterinary microbiology*, *90*(1-4), 281-297.

Kerkan, A., Banerjee, S., & Martin, D. (2021). Unpublished data.

Murrell, T. G. C., & Matthews, B. J. (1990). Multiple sclerosis—One manifestation of neurobrucellosis? *Medical hypotheses*, *33*(1), 43-48.

Pappas, G., Akritidis, N., Bosilkovski, M., & Tsianos, E. (2005). Brucellosis. *N Engl J Med*, *352*, 2325-2336.

Roop, R. M., Barton, I. S., Hopersberger, D., & Martin, D. W. (2021). Uncovering the Hidden Credentials of Brucella Virulence. *Microbiology and Molecular Biology Reviews*, *85*(1), e00021-19.

Solera, J., Lozano, E., Martínez-Alfaro, E., Espinosa, A., Castillejos, M. L., & Abad, L. (1999). Brucellar spondylitis: review of 35 cases and literature survey. *Clinical infectious diseases*, *29*(6), 1440-1449.

Yagupsky, P., & Baron, E. J. (2005). Laboratory exposures to brucellae and implications for bioterrorism. *Emerging infectious diseases*, *11*(8), 1180.